Histol Histopathol (2019) 34: 275-286

http://www.hh.um.es

Histology and Histopathology

From Cell Biology to Tissue Engineering

Multichromatic TTF staining characterizes cartilage matrix in osteoarthritis and bone development

Yu Feng[1]*, Zhe Cai[2,3,4]*, Wing ki Cheung[4], Kedi Yang[4], Lei Xu[4,5], William Weijia Lu[4,6], Haibo Yang[1] and Kwong-Yuen Chiu[4]

[1]Department of Traumatology, General Hospital of Ningxia Medical University, Yinchuan, [2]The Joint Center for Infection and Immunity; 1. Guangzhou Institute of Pediatrics, Guangzhou Women and Children's Medical Center, Guangzhou; 2. Institute Pasteur of Shanghai, Chinese Academy of Science, Shanghai, [3]Department of Pathology, The Second Affiliated Hospital of Guangzhou Medical University, The Guangzhou Medical University, Guangzhou, [4]Department of Orthopaedics and Traumatology, Li Ka Shing Faculty of Medicine, The University of Hong Kong, Hong Kong, [5]Department of Biomedical Engineering, Southern University of Science and Technology and [6]Shenzhen Institutes of Advanced Technology, Chinese Academy of Science, Shenzhen, China

*: These authors contributed equally to this work

Summary. Various histological staining methods have been explored to detect the joint lesions in osteoarthritis (OA), but these histological stains cannot comprehensively present the comparatively complex structures of articular cartilage in knee OA. In addition, no integrated histological staining method can be used to evaluate efficiently both the subzone region and matrix composition in cartilage containing tissues. Therefore, in this study, a novel multichromatic staining method termed TTF staining, using Toluidine Blue (T), Tartrazine (T) and Fast Green (F) sequential combined staining for histological analysis, has been exploited to characterize the changes of matrix components and contents in cartilage during OA and in the bone development. This specific TTF staining profile can be used to differentiate the major compartments of knee joint region, including the synovium, meniscus, multiple subzones of cartilage and subchondral bone. An anterior cruciate ligament transection induced OA model in rat has been established to profoundly present the alterations of glycosaminoglycans in cartilage degeneration by TTF staining profile. The changes of TTF staining profile in the chondrification and ossification centers of the postnatal rat knee joint indicate the developmental features of cartilage matrix during the growth of bone. In summary, we have developed an effective histological staining method that enables us to identify the subzones of cartilage in detail and to define the matrix features of bone development. Therefore, finally using this new TTF staining method may help us to exploit a histopathological grading system to assess cartilage lesions in clinical disease.

Key words: Osteoarthritis, Articular cartilage, Subchondral bone, Matrix, TTF staining

Offprint requests to: Dr. Zhe Cai, Floor 13th, 9 Jinsui Road, Guangzhou Institute of Pediatrics, Guangzhou Women and Children's Medical Center, Guangzhou, China. e-mail: caifranklin@163.com

DOI: 10.14670/HH-18-044

Introduction

Cartilage is a connective tissue and can be categorized into three types according to the matrix components and contents. The first one is hyaline cartilage, which mainly contains type-II collagen and glycosaminoglycan like chondroitin sulphate, and can be found in joint and rib tissues. The second one is elastic cartilage, which contains elastic fiber and type-II collagen, and is presented in ear and epiglottis. The last type is fibrocartilage, which contains both type-I and -II collagens, and is mainly observed in meniscus and intervertebral disc (Zhang et al., 2009).

Articular cartilage is mainly composed of extracellular matrix (ECM) and chondrocytes, and is found in various joints (Sophia et al., 2009). The major components of ECM include type-II collagen for elastic property and aggrecan for water-holding capacity. Due to lack of blood vessels in articular cartilage, it is also a poor self-repair tissue (Sophia et al., 2009). It has two main functions: lubrication and distribution of mechanical load bearing across joint surface (McNary et

al., 2012). There are four subzones in articular cartilage (Sophia et al., 2009). The first layer is the superficial zone which takes up 10-20% of the articular cartilage. The upper layer protects deeper layers from shear stresses. It contains a large number of chondrocytes and type-II and -IV collagen fibers which are aligned parallel to the surface. The second layer, making up 40-60% articular cartilage, is the middle zone. It contains regular spherical chondrocytes, proteoglycans and thick collagen fibers which are aligned obliquely. The deep zone, the third layer, is composed of 30% of the cartilage. It consists of collagen fibers, proteoglycans and chondrocytes. These chondrocytes are arranged in columnar orientation and are perpendicular to the joint surface. The collagen fibers are arranged in parallel near to the chondrocytes, and the large amount of proteoglycans contribute a great resistance to compressive forces. The last layer of articular cartilage is calcified zone which connects cartilage and bone by fixing the collagen fibers to subchondral bone (Sophia et al., 2009).

Cartilage degeneration occurs mainly due to the unbalanced mechanical stress loading at morbid status and aging (Buckwalter and Mankin, 1998). As age increases, chondrocytes will change distribution and concentrate into the deeper layers of cartilage, but the total number remains the same. At the same time with increasing age, hydration effects will be decreased which leads to an increase in compressive stiffness (Sophia et al., 2009). Abnormal stress on cartilage will induce a production of inflammatory cytokines which can stimulate the following production of matrix metalloproteinase. Then the metalloproteinase will medicate the breakdown of cartilage (Brandt et al., 2008). It is also found that cartilage matrix loss is more obvious in the central region than lateral and medial region due to a heavy load at the central region of tibial plateau in osteoarthritis (OA) (Andriacchi et al., 2004). Due to the poor self-repair ability of cartilage, persistent degeneration of cartilage without a well-established repair will eventually exacerbate the OA progression.

OA is a group of overlapping distinct diseases which affect the entire joint, including the subchondral bone, cartilage, ligaments, capsule, synovial membrane, and periarticular muscles (Buckwalter et al., 2013). Risk factors include age, gender, prior joint injury, obesity and genetic predisposition. It is characterized by the articular cartilage degradation and subchondral bone sclerosis and thickening (Goldring, 2012). During the OA progression, due to the changes of composition and organization in chondrocyte, a decrease of the mechanical properties and structural integrity in cartilage has occurred. Meanwhile, there can be observed an abnormal increase in subchondral bone turnover and in secretion of inflammatory cytokines. These secreted cytokines which are alkaline phosphatase, matrix metalloproteinase, type-I collagen and regulatory factors lead to the un-mineralized and immature new bone formation (Sharma et al., 2013).

Anterior cruciate ligament transection (ACLT) is the most commonly established method to induce an OA model. The rupture of ACL will first directly cause joint destabilization. In this situation due to the unstabilized mechanical loading, articular cartilage will be degraded, and thus eventually lead to OA (Kuyinu et al., 2016). Compared to other OA model like DMM (the destabilization of the medial meniscus), the development of OA lesions are slower than ACLT induced OA (Kuyinu et al., 2016). For this reason, we have used the ACLT induced OA model in rat to profoundly observe the pathological changes of articular cartilage through a new staining method termed TTF staining (TTF is derived from the first capital letter of each staining reagent including Toluidine Blue, Tartrazine solution and Fast Green).

We have established this staining approach through sequential staining in cartilage with Toluidine Blue, Tartrazine and Fast Green. Toluidine Blue mainly stains glycosaminoglycans, a major component of cartilage and collagenous fibers. In addition, it also has a quite high affinity for sulfated glycosaminoglycans like heparin in cartilage (Schmitz et al., 2010). Tartrazine interacts preferentially with mucin-associated ECM, which is secreted from fibroblasts in woven bone and intestine (Leung et al., 2009). As a counterstain of Toluidine Blue and Tartrazine, Fast Green stains the glycoprotein-rich rigid structures such as cellulose, cytoplasm and bone (Leung et al., 2009).

In this study, we have elucidated a new multichromatic TTF staining protocol for histological assessment of cartilage containing tissues by examining the alterations of structure and matrix in rat samples. Our aim is using the TTF staining method, we can expect the distinct differences of bone and articular cartilage matrix, categorize the characteristic zones in articular cartilage, and verify the degeneration of articular cartilage in the pathological status like ACLT induced OA.

Materials and methods

ACLT model

The Ethics Committee On The Use Of Live Animals In Teaching & Research of The University of Hong Kong approved all the protocols and procedures in this study. The new born Sprague-Dawley (SD) rats from Day 0 to Day 5 were sacrificed to collect cartilage containing tissues. The 8-week-old SD rat (250-260 g/rat) were bred and maintained under specific pathogen-free conditions in the Laboratory Animal Unit Center of The University of Hong Kong. Ten female SD rats were randomly assigned into the ACLT group (n=5) and the Sham group (with the same operation but non-ACLT surgery, n=5). The ACLT operation was performed only on the right hind limb to induce the model of post-traumatic knee OA through following a well-established protocol as previously described

(Appleton et al., 2007a,b,c; McErlain et al., 2008, 2012). All samples were collected at 3-month post-surgery for histopathological evaluation.

Histology

To verify the effect of TTF staining approach, we have harvested cartilage containing tissues like ear, finger, rib, trachea and knee joint from SD rat. To investigate the cartilage changes in the development of bone during postnatal growth, we harvested knee joint from SD rat at birth (Day 0), 1 day, 3 days and 5 days of age. The knee joints from rats in Sham and ACLT groups were harvested to evaluate the pathological degeneration of articular cartilage (Fig. 1 and 2). All tissues were fixed in 4% paraformaldehyde and were decalcified in 0.5 M EDTA-Na_2 (pH 7.5) at room temperature. They were dehydrated in the gradient concentrations of ethanol, then cleared in xylene, and lastly embedded in paraffin. The embedded samples were sectioned into 5 μm using Leica RM2135 microtome (Leica Microsystems; Wetzlar, Germany).

TTF staining

TTF Staining is a multichromatic histological staining approach, which is developed to investigate cartilage containing tissues like ear, finger, rib, trachea and joint through sequential staining with Toluidine Blue (0.04% w/v in 0.1 M sodium acetate), Tartrazine solution (0.025% w/v in 2.5% acetic acid) and 0.1% Fast Green in deionized water. The five-micron-thick serial paraffin sections were deparaffinized in xylene and rehydrated in gradient alcohol, and stained with 0.04% Toluidine blue solution for 2 mins, followed by 0.025% Tartrazine solution for 20 sec, and finally counterstained with 0.1% Fast Green for 20 sec. The sections were rinsed in distilled water for 2 mins between each staining. Finally, the sections were submerged in distilled water for 5 mins. After air drying, the slides were submerged in xylene before being mounted in Fisher Chemical™ Permount™ Mounting Medium (Fisher Scientific Company LLC., Pittsburgh, PA, USA). The TTF staining protocol is shown in Table 1.

Micro-CT analysis

Collected knee joints were fixed in 10% neutral buffered formalin and scanned using a high resolution micro-CT system (model 1076, SkyScan, Kontich, Belgium). Three hundred and twenty-nine projections for each sample were produced with the following settings: Isotropic voxel 17.3 μm, voltage 100 kV, current 100 mA, and exposure time 320 ms, frame averaging 2, beam filtration filter 1.0 mm aluminum. After scanning, the data sets were then reoriented using DataViewer (version 1.4.4.0, SkyScan) to analyze in the sagittal plane. Binarization of the images with a global thresholding of gray levels (60-252), the calculation of morphological parameters was carried out with the CTAn software (version 1.13.2.1, SkyScan). The trabecular bone volume fraction (BV/TV, %), degree of anisotropy (DA), trabecular number (Tb.N), trabecular thickness (Tb.Th, mm), trabecular bone pattern factor (Tb.Pf, 1/mm), structure model index (SMI), trabecular separation (Tb.Sp, mm) and trabecular bone total porosity (Po(tot), %) were measured (Hahn et al., 1992). Bone mineral density (BMD) (g/cm^3) was calibrated by using the attenuation coefficient of two hydroxyapatite phantoms with defined mineral density of 0.25 and 0.75 g/cm^3. Additionally, for analysis of subchondral trabecular bone degeneration, a cuboid of load bearing region in the middle area of medial tibial close to subchondral bone plate was selected as Region of Interest (yellow rectangle area, Fig. 3A-B) in size of 0.692 x 0.346 x 0.692 mm^3 to do the three-dimensional (3D) reconstruction (Fig. 3C-D) by SkyScan NRecon software (version 1.6.8.0, SkyScan).

Table 1. TTF Staining Protocol.

Solutions	0.04% Toluidine blue	Prepare in 0.2 M acetate buffer, mix on magnetic stirrer and filter before use
	0.025% Tartrazine	Tartrazine solution (0.025% w/v) in 0.25% acetic acid
	0.1% Fast green	0.1 g Fast green dissolved in 100ml distilled water and filter before use
Staining procedure	solution	Time
	1 Xylene	5 mins
	2 Xylene	5 mins
	3 100% Ethanol	3 mins
	4 95% Ethanol	3 mins
	5 75% Ethanol	3 mins
	6 Distilled water	3 mins
	7 Toluidine blue	2 mins
	8 Distilled water	2 mins
	9 Tartrazine	20 secs
	10 Distilled water	2 mins
	11 Fast green	20 sec
	12 Distilled water	5 mins
	13 Xylene	5 mins
	14 Mount with mounting solution	

Statistical analysis

Statistical analysis of the parameters of subchondral trabecular bone at the medial tibial was described of the knee joint from right hind limb in Sham and ACLT groups. Results were expressed as mean ± standard error mean for normally distributed data. Since the sample size is small (n=5/group), non-parametric Mann-Whitney U-test was performed for comparing the differences between two groups. All hypotheses were 2-tailed, and p values<0.05 were considered significant. Analysis was performed using GraphPad Prism (version 6.0 for Windows, GraphPad Software, La Jolla, CA, USA).

Results

Defining cartilage structure from different tissues by TTF staining

We first tested whether the TTF Staining method could define the structure of cartilage in different organs

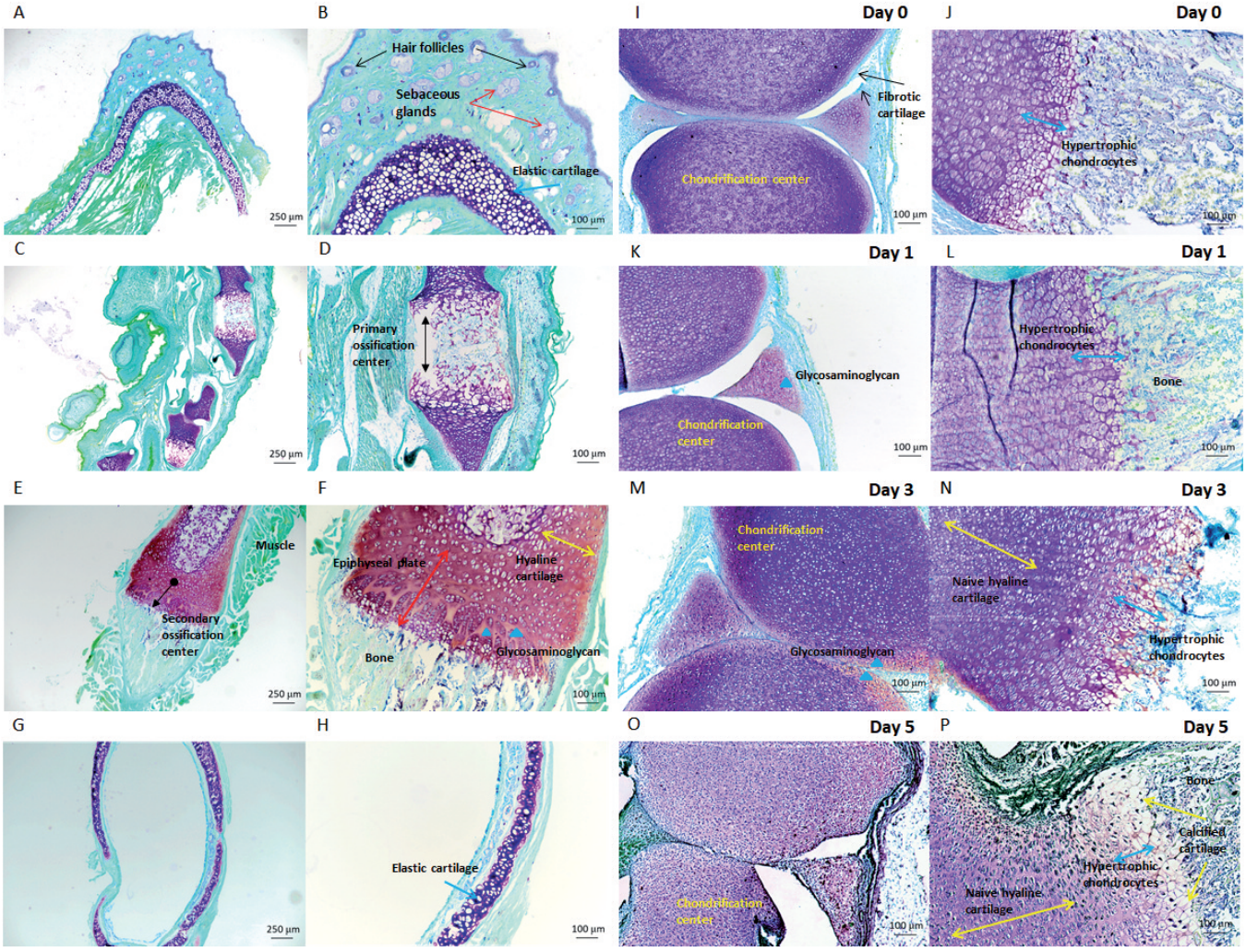

Fig. 1. Identifying cartilage from different tissues by TTF Staining. **A, B.** The representative images show the histological sections of rat ear. The black arrow points to hair follicles. The red arrow points to sebaceous glands. The blue arrow points to elastic cartilage. **C, D.** The representative images show the histological sections of rat finger. The black double arrow points to the primary ossification center. **E, F.** The representative images show the histological sections of rat rib. **E.** The unidirectional black arrow points to the secondary ossification center. The muscle fiber beside the rib is stained in green. **F.** The red double arrow points to the epiphyseal plate closely adjacent bone matrix. The yellow double arrow points to hyaline cartilage. The blue triangle points to the glycosaminoglycan. **G, H.** The representative images show the histological sections of rat trachea. The blue arrow points to the elastic cartilage. **I-P.** The representative images show the histological sections of the knee joint from 0 to 5-day-old rat. **I.** The black arrow points to the fibrotic cartilage. **J, L, N, P.** The blue double arrow points to the hypertrophic chondrocytes. **K, M.** The blue triangle points to the glycosaminoglycan. **N, P.** The yellow double arrow points to the naive hyaline cartilage. **P.** The yellow arrow points to the calcified cartilage. Scale bars: A, C, E, G, I-P, 100 μm; B, D, F, H, 250 μm.

such as ear, finger, rib, trachea and joint. From the results of staining, we found with TTF staining most of the outer layer tissues around the cartilage tissues were stained in blue, greenish blue or green. For example, the bone marrow observed in primary ossification center was stained in light blue (Fig. 1D), and the muscle fiber beside the rib was stained in green (Fig. 1E). However, the cartilage matrix was stained in purple color due to the intense Toluidine Blue. Therefore, we could clearly define the different tissues by different colors.

For instance, the auricle tissue, which was composed of hair follicles, sweat and sebaceous glands and supporting structure of elastic cartilage (Fig. 1A-B), could be identified by TTF staining. The hair follicle (block arrow pointed) was stained in light purple and the sebaceous gland (red arrow pointed) was stained in light gray (Fig. 1B). Lots of proteoglycans (blue arrow pointed purple color) around the dense chondrocytes in ear elastic cartilage (Fig. 1B) and trachea hyaline cartilage (Fig. 1H) could be obviously distinguished from the epithelium and secretion glands which were stained in blue color, and distinguished from the connective tissues which were stained in greenish blue or green color. Furthermore, we could identify an obvious primary ossification center (black double arrow pointed) in diaphysis of finger (Fig. 1D), the fibrotic cartilage (black arrow pointed) covered on the surface area of articular cartilage and meniscus (Fig. 1I), and the epiphyseal plate (red double arrow pointed) covered with glycosaminoglycan (blue triangle pointed) on its surface as a secondary ossification center (unidirectional black arrow pointed) between hyaline cartilage (yellow double arrow pointed) and new bone in rib (Fig. 1E-F). But we didn't find the undifferentiated chondrification center in this tissue. Meanwhile, according to the process of endochondral bone formation, some of the columnar prechondrocytes in epiphyseal plate could be differentiated to be hypertrophic chondrocytes. Then these hypertrophic chondrocytes could be calcified to form the osteoid islands, and finally complete the process of endochondral bone formation. From the result of completely calcified cartilage (yellow arrow pointed) which was stained in light blue color and observed between hyaline cartilage and formed bone (greenish-blue) in 5-day-old rat (Fig. 1P), we could believe the process of bone formation could be clearly identified by the TTF staining approach.

Cartilage continual change and endochondral bone formation during bone development

Interestingly, hyaline cartilage from rib tissue was stained in wine-red, but the same cartilage matrix like glycosaminoglycan (blue triangle pointed) was clearly observed in some parts around the hypertrophic chondrocytes (blue double arrow pointed) at epiphyseal plate, meniscus and surface area of articular cartilage in 3-day-old rat (Fig. 1M-N). This means that they might have the same composition of molecules like keratan sulfate and heparin. However, most of the cartilage matrix around chondrocytes in these tissues was stained in purple color, especially the chondrification center and naive hyaline cartilage area (Fig. 1I-P). This was confirmed in the bone development of newborn rat from Day 0 to Day 5 (Fig. 1I-P). All of these proved that the ingredients of cartilage matrix in the area of chondrification center were different from those around hypertrophic chondrocytes. This means that through the TTF staining approach, the proliferative chondrogenitor cells in chondrification center could be distinguished from those differentiated hypertrophic chondrocytes who will eventually be calcified to be osteoid. Then we could

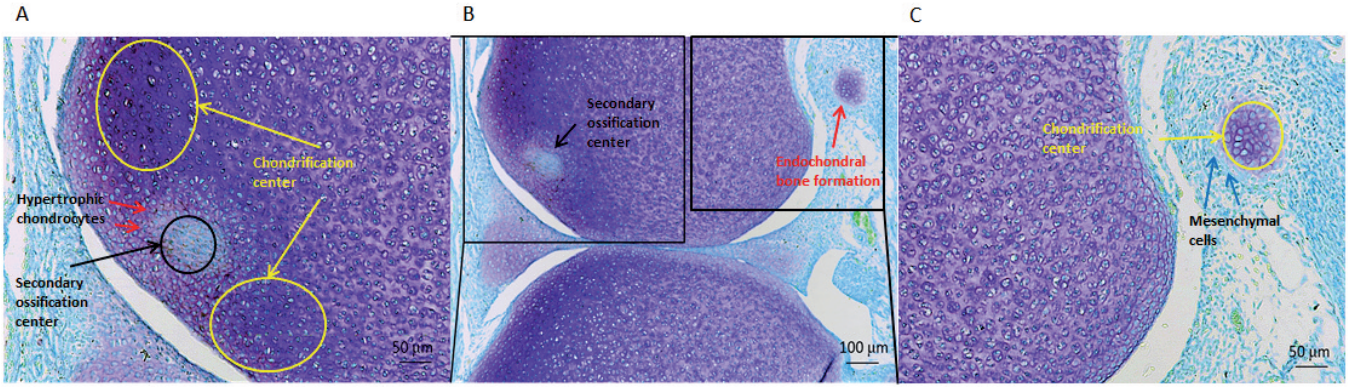

Fig. 2. Identifying the site of endochondral bone formation in articular cartilage by TTF Staining. **A-C,** The representative images show the histological sections of the knee joint in 0-day-old rat. **A.** The red arrow points to the hypertrophic chondrocytes. The yellow circle area pointed by yellow arrow shows the chondrification center. The black circle area pointed by black arrow shows the secondary ossification center. **B.** The black rectangle shows the magnified area. The red arrow points to the chondrogenic site of endochondral bone formation. The black arrow points to the secondary ossification center. **C.** The yellow circle area pointed by yellow arrow shows the chondrogenic center. The blue arrow points to the mesenchymal cells. Scale bars: A, C, 50 μm; B, 100 μm.

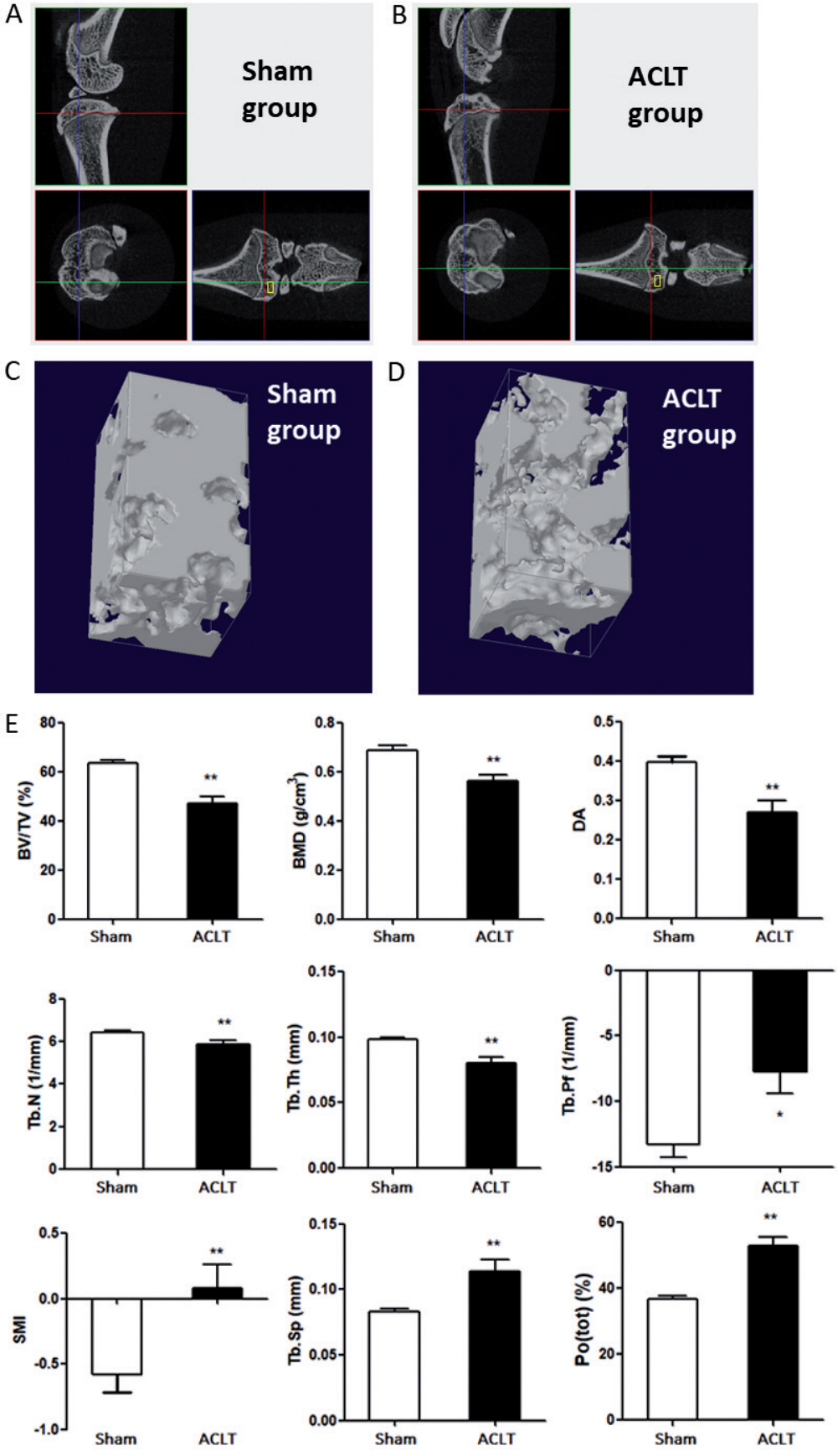

Fig. 3. Micro-architectures of subchondral bone in the Sham and anterior cruciate ligament transection (ACLT) groups. **A, B.** 3-view micro-CT images of knee joint from right hind limb (sagittal view) in the Sham and ACLT groups. The yellow rectangle shows the range of interest (ROI) for three-dimensional (3D) reconstruction and micro-architectural assessment. **C, D.** 3D reconstruction images of the ROI show the load bearing region of subchondral trabecular bone at medial tibia in Sham and ACLT groups. **E.** The Bar charts show the mean values of micro-architectural parameters of medial tibial subchondral bone, n=5/group. Differences between two groups are compared by Student's t-test. (* $p<0.05$, ** $p<0.01$; ACLT group vs. Sham group).

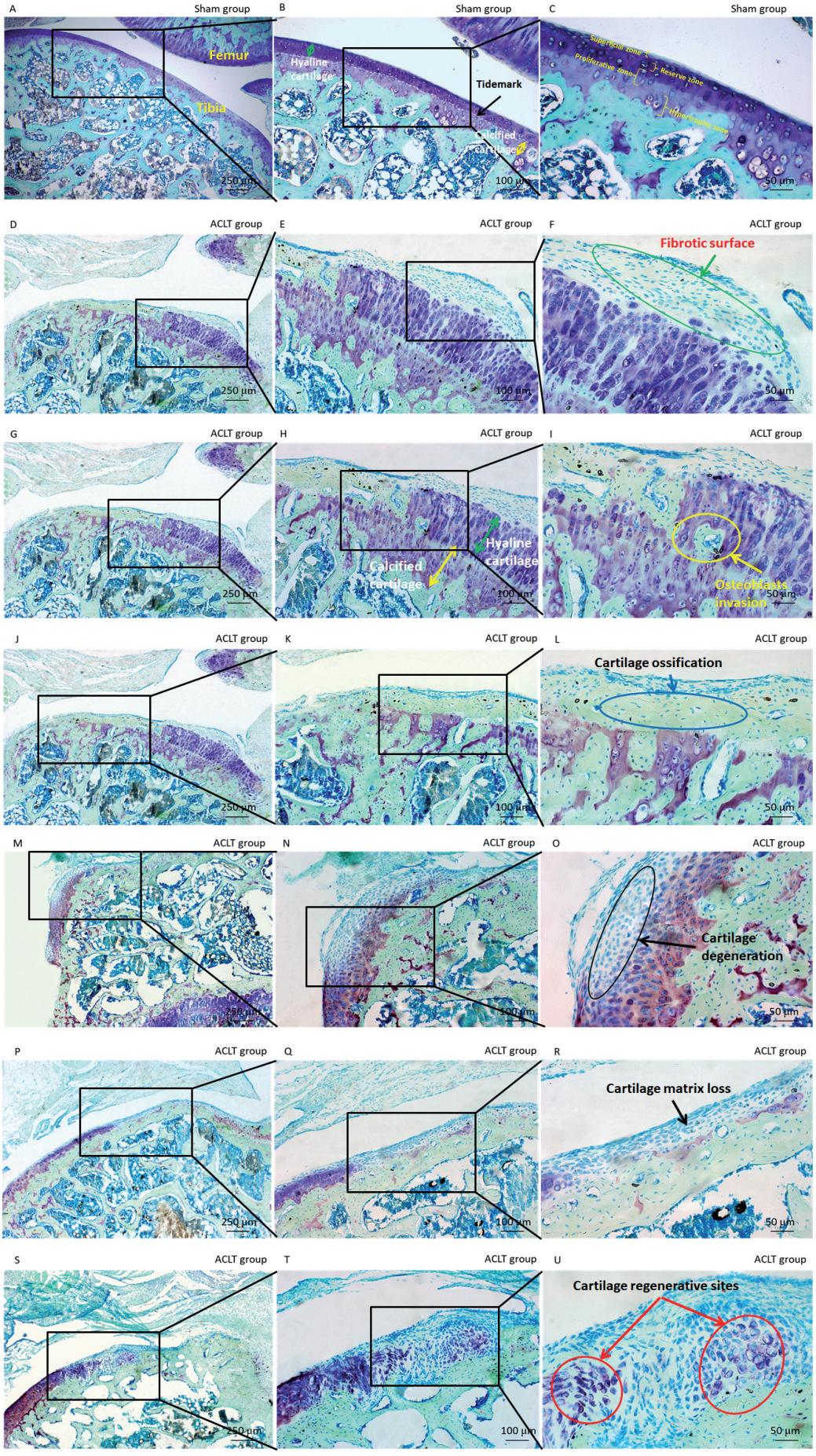

Fig. 4. Histological images of medial tibial plateau in the Sham and ACLT groups by TTF Staining. The representative histological images show the Toluidine Blue, Tartrazine solution and Fast Green sequentially stained medial tibial plateau area in the Sham group **(A-C)** and ACLT group **(D-I)**. The black rectangles show the magnified areas. **B.** The green double arrow points to the hyaline cartilage (HC) area, and the calcified cartilage (CC) area pointed by yellow double arrow in the Sham group. The black arrow pointing to the white dash line shows the tidemark between HC and CC. **C.** The yellow parentheses show four subzones of articular cartilage (superficial, reserve, proliferative and hypertrophic zone). **F.** The green circle area pointed by green arrow shows the fibrotic surface of articular cartilage. **H.** The green double arrow points to the thinner HC area and the yellow double arrow points to the thicker CC area in ACLT group. **I.** The yellow circle area pointed by yellow arrow shows the osteoblasts invasion. **L.** The blue circle area pointed by blue arrow shows cartilage ossification area. **O.** The black circle area pointed by black arrow shows cartilage degenerative area. **R.** The black arrow points to the matrix lost area of cartilage. **U.** The red circle area pointed by red arrow shows cartilage regenerative sites. Scale bars: A, D, G, J, M, P, S, 250 µm; B, E, H, K, N, Q, T, 100 µm; C, F, I, L, O, R, U, 50 µm.

presume that some of the chondrogenitor cells might be differentiated to be hypertrophic chondrocytes. Thus these cells would be fibration and calcified to form the secondary ossification center during the bone development. This was confirmed in the bone development from 0-day-old rat (Fig. 2A,B). We have found that the chondrogenitor cells (yellow arrow pointed yellow circle area) which stained in dark purple aggregated near to the hypertrophic chondrocytes (red arrow pointed) who surrounded the fibrocartilage (light blue) in the secondary ossification center (black arrow pointed black circle area, Fig. 2A).

Besides distinguishing the chondrification center and secondary ossification center, we also observed the chondrogenic site of endochondral bone formation (red arrow pointed, Fig. 2B). The flattened fusiform cells (blue arrow pointed) which were defined as mesenchymal cells surrounded the aggregated chondrogenic cells (purple color, Fig. 2C). These aggregated chondrogenic cells as a chondrification center (yellow arrow pointed yellow circle area) would differentiate to be growth plate through hypertrophic differentiation, and then with the vascular invasion, osteoprogenitor cells would differentiate to form a periosteum and complete the process of endochondral bone formation (Ornitz and Marie, 2002).

Sign of cartilage degeneration shown by TTF staining

Although TTF staining could clearly identify the structure of cartilage in different organs and tissues, especially, clearly define the ossification center, chondrification center and the process of endochondral bone formation during the development of bone, we would like to confirm whether this staining approach could clearly reflect the cartilage degeneration on the pathological status of OA via using a rat ACLT model. Therefore, at 3-month post-surgery of ACLT, when compared with Sham group (Fig. 3A,C), we found obvious bone mass loss of subchondral trabecular bone shown in 3-view (Fig. 3B) and 3D reconstruction images (Fig. 3D), which were reflected by the obvious changes of subchondral bone parameter at the load bearing area of medial tibial in ACLT group (Fig. 3E). Specifically, in the ACLT group, the parameters of trabecular bone microstructures had a significant decrease, such as BV/TV, BMD, DA, Tb.N and Tb.Th, as well as a significant increase like Tb.Pf, SIM, Tb.Sp and Po(tot), which implied an accelerated damage of subchondral trabecular bone (Fig. 3E).

In accordance with these findings, the TTF staining of articular cartilage was shown in Figure 4. In the Sham group, the well-defined structure of articular cartilage could be observed (Fig. 4A-C). There was a clear tidemark (black arrow pointed white dash line) between the thicker hyaline cartilage area (green double arrow pointed) and the thinner calcified cartilage area (yellow double arrow pointed) at the medial tibial side in the Sham group (Fig. 4B). Moreover, the intact articular cartilage contained four layers of well-arranged chondrocytes and their ECM like collagens, glycosaminoglycans and glycoproteins. Through the TTF staining, we could methodically identify the well-arranged chondrocytes in four layers (superficial, reserve, proliferation and hypertrophy zone) of articular cartilage (Fig. 4C). However, compared to the Sham group, there were varying degrees of cartilage degradation in the ACLT group (Fig. 4D-U). For example, we could observe the thicker fibrotic superficial zone (green arrow pointed green circle area) shown in Fig. 4F, the thicker calcified cartilage area (yellow double arrow pointed), the thinner hyaline cartilage (green double arrow pointed) shown in Fig. 4H, the osteoblasts invasion in cartilage (yellow arrow pointed yellow circle area) shown in Fig. 4I, the completely lost ingredients of cartilage matrix (without purple color stained) shown in Fig. 4R, the cartilage regenerative sites (red arrow pointed red circle area, Fig. 4U) during the gradual degradation of intact cartilage (black arrow pointed black circle area) shown in Fig. 4O, and finally the complete ossification of cartilage (blue arrow pointed blue circle area) shown in Fig. 4L. Thus, these results suggested that the TTF staining method could easily reflect the degrees of cartilage degeneration in OA. We also found no clear boundary between ossified cartilage and subchondral bone plate in Fig. 4L, and found a thicker subchondral bone plate under the degenerated cartilage, cartilage matrix loss area and ossified cartilage. This might be a predictive sign for subchondral bone plate sclerosis. However, the characteristics in the subchondral bone via TTF staining need to be further investigated.

Advantages of TTF staining

Generally, Masson's trichrochome staining was usually used to identify the collagenous fibers from muscle fibers. Clinically, Hematoxylin and Eosin (H&E) staining was the most commonly used staining method for every tissue. Although these traditional staining methods like Masson's trichrochome staining, H&E staining and Safranin-O and Fast Green (S&F) combined staining could easily differentiate the cartilage, bone and peripheral tissues, the subzones and microstructures of cartilage still need to be identified clearly, especially through a spectrum of colors. Therefore, using the TTF staining approach, we had clearly observed the subzones and microstructures of cartilage which could be identified via a spectrum of colors (Fig. 5M-O), when compared to the single stain like Toluidine Blue (Fig. 5A-C) or Fast Green (Fig. 5D-F), as well as the combined double stains including Toluidine Blue and Tartrazine solution (Fig. 5G-I), Toluidine Blue and Fast Green (Fig. 5J-L), S&F (Figure. 5P-R) and H&E (Figure. 5S-U) in staining of ACLT knee joints. Additionally, through the spectrum of colors in TTF staining, we not only observed the changes of cartilage matrix in the process of bone growth, but we also

profoundly observed the pathological changes of articular cartilage in OA (Fig. 1 and 4). However, because TTF staining is a new staining method to identify the resolution of microstructures in articular cartilage, how to provide a proper modified Mankin or OARSI scores needs to be further investigated.

Discussion

Principle rationale of TTF staining

In this study, we have reported a novel histological staining approach using a combination of three chemical dyes with affinity for proteoglycans to assess the properties of structure and matrix in the cartilage containing tissues. The principle rationale of this staining approach is that the acidic proteoglycans like hyaluronan in cartilage can firstly make a metachromatic chemical reaction with Toluidine Blue to be purple color. Subsequently, the bone matrix and fibrous tissues are shortly counterstained with acidic Tartrazine solution to be light yellowish green color. However, due to the gradual acidification of keratan sulfate and heparin in the acidic environment, the hypertrophic chondrocytes and some surface area of articular cartilage with large amount of heparin are counterstained to be wine-red color (Fig. 1M,N). The resultant color in the cartilage with a mixture of acidic and neutral glycosaminoglycans is reflected by the dominant functional group. Finally, with neutral Fast Green counterstained, the bone matrix and fibrous tissues become greenish blue and yellowish green color, respectively (Leung et al., 2009). Noteworthy, the nuclear acid, collagen in fibrotic cartilage and completely calcified cartilage are stained in blue color by TTF staining approach (Fig. 1). In the bone marrow, the osteoblasts and osteocytes are reflected via nucleus staining to be blue color, which can be clearly distinguished from erythrocytes stained in yellowish green color.

Unique resolution of articular cartilage structure

With the TTF staining method, the structures in articular cartilage can be identified via a spectrum of colors, which for us, is the first time to demonstrate the differentiation of bone and articular cartilage matrix, the categorization of the characteristic zones in articular cartilage, the clear visualization of the epiphyseal plate and endochondral bone formation site, and the distinct differentiation of the primary (initiate from hyaline cartilage to form osteoid in diaphysis) and secondary ossification center (initiate from fibrotic cartilage to form calcified cartilage in epiphysis) from chondrification center (Fig. 1). Furthermore, this method enables us to distinguish the superficial cartilage from the outer fibers, and with an extended analysis enables us to further define the different cartilages such as elastic cartilage, fibrocartilage and hyaline cartilage based on the staining of cell types and cartilage matrix (Table 2). Pritzker and his co-authors have reported three well-

Table 2. TTF staining profile of joint in the bone development under staining protocol.

Compartment	Subdivision	Matrix color	Cell color (pericellular)
Primary ossification center	Osteoid and bone	Yellowish green	Blue (nucleus)
	Bone marrow	Colorless	Blue (nucleus) and yellow (erythrocytes)
Epiphyseal plate	Hyaline cartilage	Purple	Blue (nucleus) and purple (cytoplasm)
	Columnar arrayed chondrocytes	Wine-red and purple	Blue (nucleus) and purple (cytoplasm)
Secondary ossification center		Light blue	Blue
Chondrification center		Purple	Blue (nucleus) and purple (cytoplasm)
Cartilage	Elastic cartilage	Dark purple	Purple (cytoplasm)
	Fibrocartilage	Blue	Blue
	Naive hyaline cartilage	Purple	Blue (nucleus) and purple (cytoplasm)
	Calcified cartilage	Light blue	Blue (nucleus) and colorless (cytoplasm)
	Superficial cartilage	Wine-red and light blue	Light blue
	hypertrophic cartilage	Wine-red	Blue (nucleus) and colorless (cytoplasm)

Table 3. TTF staining profile of degenerative articular cartilage in OA under staining protocol.

Compartment	Subdivision	Matrix color	Cell color (pericellular)
Trabecular bone		Yellowish green	Blue
Subchondral bone plate		Yellowish green	Blue
Obscured tidemark		Colorless	Nil
Degenerative articular cartilage	Fibrotic superficial zone	Greenish blue	Blue
	Degenerative reserve zone	Purple	Blue (nucleus) and purple (cytoplasm)
	Reduced proliferative zone	Purple	Blue (nucleus) and purple (cytoplasm)
	Expanded hypertrophic zone	Light wine-red	Blue (nucleus) and purple or Wine-red (cytoplasm)

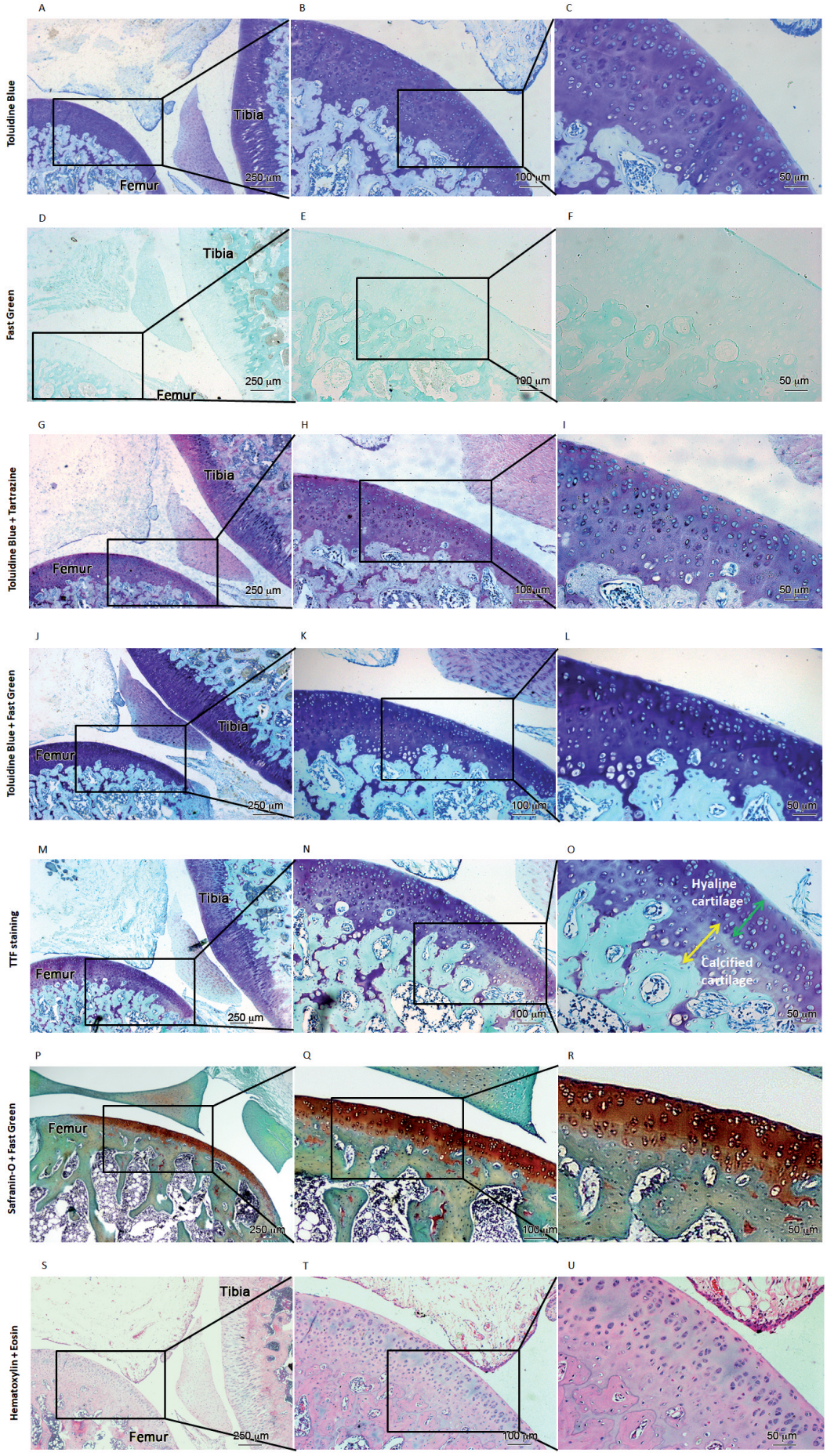

Fig. 5. Histological images of knee joints from ACLT rat with single staining, traditional staining and TTF staining. The representative histological images of knee joint tissues from ACLT rat show the single staining with Toluidine Blue **(A-C)** and Fast Green **(D-F)**; the double staining combined with Toluidine Blue and Tartrazine solution **(G-I)**; the double staining combined with Toluidine Blue and Fast Green **(J-L)**; the TTF sequential staining combined with Toluidine Blue, Tartrazine solution and Fast Green **(M-O)**; and traditional double staining combined with Safranin-O and Fast Green **(P-R)**; and combined with Hematoxylin and Eosin **(S-U)**. The black rectangles show the magnified areas. **F.** The green double arrow points to the hyaline cartilage area and the yellow double arrow points to the calcified cartilage area of articular cartilage. Scale bars: A, D, G, J, M, P, S, 250 μm; B, E, H, K, N, Q, T, 100 μm; C, F, I, L, O, R, U, 50 μm.

ordered zones of articular cartilage according to the appearance of cellular array and matrix (Pritzker et al., 2006). In this study, we have demonstrated that using our TTF staining approach four clearly arranged subzones can be defined in the knee cartilage of normal (Fig. 4C) and ACLT- induced OA (Table 3). In the hypertrophic zone, the hypertrophic chondrocytes which identified via wine-red color suggest a conversion of ECM composition like glycosaminoglycan. These results may reflect a response to the gene modulation for the differentiation of chondrocytes (Kuiper and Sharma, 2015).

Analysis of the cartilage degeneration in OA by TTF Staining

The articular cartilage matrix preferentially reacts with Toluidine Blue, when compared to the other joint compartments. This feature enables us to present the obvious changes of articular cartilage matrix during cartilage degeneration by using TTF staining. From our analysis of the ACLT induced OA model in rat, there are comprehensive alterations of cartilage matrix and cells, as well as the changes of subchondral bone in OA. According to previous studies (Batiste et al., 2004; Meyer et al., 2008; Intema et al., 2010), the temporal bone mass loss of subchondral bone in the development of OA was a critical step to exacerbate the deterioration of subchondral bone, which would lead to an unstable mechanical loading status in the progression of OA and induce the degeneration of overlying articular cartilage. Moreover, during the development of OA, the rapid subchondral trabecular bone losses following traumatic injuries and then the subchondral bone sclerosis at the advanced stage of OA are the well-defined hallmarks of this disease (Chen et al., 2018). Therefore, from our micro-CT results on 3-month post-surgery of ACLT, the traumatic OA may not reach the advanced stage. Thus, the subchondral bone sclerosis may occur mainly at the late stage of ACLT induced OA. In this study, the TTF staining profiles present that the losses of intensity and extent of the distribution of Toluidine blue stained articular cartilage are related to the severity of cartilage degeneration. We propose that these changes are related to a gradual transformation of glycosaminoglycan components, followed by the complete breakdown of matrix, and to the calcification and ossification initiated by the cartilage degeneration. The changes of glycosaminoglycan components in the degenerative cartilage announced in some human OA samples and animal progressive OA models have supported our findings (Leung et al., 2009). We presume that the total content and allocation of intensely sulfated glycosaminoglycan, which prefers to interact with Toluidine Blue and Tartrazine at a low pH environment, can imply a complementary sign to the severity of cartilage degeneration. Besides, the apparent disorder of cellular array and distribution in the degenerative cartilage of OA suggests the degeneration of ECM which in turn exacerbates an aberrant metabolism in chondrocytes. Although using this ACLT induced OA model to analyze cartilage degeneration has been widely accepted (Glasson et al., 2010), whether these observations can apply to other cartilage degenerative disease in humans still needs to be further examined.

Conclusion

The TTF staining method has created a staining profile of histological structure in cartilage containing tissues especially the knee joint, which may benefit to definitely examine the useful information from these tissues to provide some possible presumptions for the pathogenesis regarding the degeneration of articular cartilage in the development of OA. In this study, the TTF staining approach not only shows the changes of cartilage matrix in the process of bone growth, but also shows the progression of articular cartilage degeneration in the pathological status like OA, which is correlated with obvious alterations of the components and contents of glycosaminoglycans. Thus, this staining method may help to develop a histopathological scoring system for the laboratory and clinical pathological application, in future.

Acknowledgements: We thank Ms. Helen Chan and Mr. Tony Liu for technical support, Mr. Boris Chan, Mr. Kedi Yang, Ms. Xin Zhong and Mr. Tianhao Sun for their efforts on the contributions of experience and the experimental support. We thank Mr. Lei Xu and Mr. Chentian Li for assistance in animal surgery and collection of animal samples. The authors acknowledge the support from Li Shu Fan Medical Foundation Endowed Professorship in Orthopaedic Surgery.

Role of the funding source: This work was supported by The Research Grant Council (RGC) Theme-based Research Scheme (TRS) funding (HKUT13-402/17-N) and the Research Grant Council of Hong Kong (RGC GRF HKU17206916) and the Shenzhen Peacock Program (No. 110811003586331).

Conflict of interest: The authors declare no conflict of interest.

References

Andriacchi T.P., Mundermann A., Smith R.L., Alexander E.J., Dyrby C.O. and Koo S. (2004). A framework for the in vivo pathomechanics of osteoarthritis at the knee. Ann. Biomed. Eng. 32, 447-457.

Appleton C.T., McErlain D.D., Pitelka V., Schwartz N., Bernier S.M., Henry J.L., Holdsworth D.W. and Beier F. (2007a). Forced mobilization accelerates pathogenesis: characterization of a preclinical surgical model of osteoarthritis. Arthritis Res. Ther. 9, R13.

Appleton C.T., McErlain D.D., Henry J.L., Holdsworth D.W. and Beier F. (2007b). Molecular and histological analysis of a new rat model of experimental knee osteoarthritis. Ann. NY Acad. Sci. 1117, 165-174.

Appleton C.T., Pitelka V., Henry J. and Beier F. (2007c). Global analyses of gene expression in early experimental osteoarthritis. Arthritis Rheum. 56, 1854-1868.

Batiste D.L., Kirkley A., Laverty S., Thain L.M., Spouge A.R. and Holdsworth D.W. (2004). Ex vivo characterization of articular

cartilage and bone lesions in a rabbit ACL transection model of osteoarthritis using MRI and micro-CT. Osteoarthritis Cartilage 12, 986-996.

Chen Y., Hu Y., Yu Y.E., Zhang X., Watts T., Zhou B., Wang J., Wang T., Zhao W., Chiu K.Y., Leung F.K., Cao X., Macaulay W., Nishiyama K.K., Shane E., Lu W.W., Guo X.E. (2018). Subchondral Trabecular Rod Loss and Plate Thickening in the Development of Osteoarthritis. J. Bone Miner. Res. 33, 316-327.

Brandt K.D., Dieppe P. and Radin E.L. (2008). Etiopathogenesis of Osteoarthritis Rheum. Dis. Clin. North Am. 34, 531-559.

Buckwalter J.A. and Mankin H.J. (1998). Articular cartilage: degeneration and osteoarthritis, repair, regeneration, and transplantation. Instr. Course. Lect. 47, 487-504.

Buckwalter J.A., Anderson D.D., Brown T.D., Tochigi Y. and Martin J.A. (2013). The roles of mechanical stresses in the pathogenesis of osteoarthritis: Implications for treatment of joint injuries. Cartilage. 4, 286-294.

Glasson S.S., Chambers M.G., Van Den Berg W.B. and Little C.B. (2010). The OARSI histopathology initiative-recommendations for histological assessments of osteoarthritis in the mouse. Osteoarthritis Cartilage 18 (Suppl 3), S17-23.

Goldring M.B. (2012). Chondrogenesis, chondrocyte differentiation, and articular cartilage metabolism in health and osteoarthritis. Ther. Adv. Musculoskelet. Dis. 4, 269-285.

Hahn M., Vogel M., Pompesius-Kempa M. and Delling G. (1992). Trabecular bone pattern factorea new parameter for simple quantification of bone microarchitecture. Bone 13, 327-330.

Intema F., Hazewinkel H.A., Gouwens D., Bijlsma J.W., Weinans H., Lafeber F.P. and Mastbergen S.C. (2010). In early OA, thinning of the subchondral plate is directly related to cartilage damage: results from a canine ACLT-meniscectomy model. Osteoarthritis Cartilage 18, 691-698.

Kuiper N.J. and Sharma A. (2015). A detailed quantitative outcome measure of glycosaminoglycans in human articular cartilage for cell therapy and tissue engineering strategies. Osteoarthritis Cartilage 23, 2233-2241.

Kuyinu E.L., Narayanan G., Nair L.S. and Laurencin C.T. (2016). Animal models of osteoarthritis: classification, update, and measurement of outcomes. J. Orthop. Surg. Res. 11, 19.

Leung V.Y.L., Chan W.C.W., Hung S.C., Cheung K.M.C. and Chan D. (2009). Matrix remodeling during intervertebral disc growth and degeneration detected by multichromatic FAST staining. J. Histochem. Cytochem. 57, 249-256.

McErlain D.D., Ulici V., Darling M., Gati J.S., Pitelka V., Beier F. and Holdsworth D.W. (2012). An in vivo investigation of the initiation and progression of subchondral cysts in a rodent model of secondary osteoarthritis. Arthritis Res. Ther. 14, R26.

McErlain D.D., Appleton C.T., Litchfield R.B., Pitelka V., Henry J.L., Bernier S.M., Beier F. and Holdsworth D.W. (2008). Study of subchondral bone adaptations in a rodent surgical model of OA using in vivo micro-computed tomography. Osteoarthritis Cartilage 16, 458-469.

McNary S.M., Athanasiiou K.A. and Reddi A.H. (2012). Engineering lubrication in articular artilage. Tissue. Eng. Part B. Rev. 18, 88-100.

Meyer E.G., Baumer T.G., Slade J.M., Smith W.E. and Haut R.C. (2008). Tibiofemoral contact pressures and osteochondral microtrauma during anterior cruciate ligament rupture due to excessive compressive loading and internal torque of the human knee. Am. J. Sports Med. 36, 1966-1977.

Ornitz D.M. and Marie P.J.. (2002). FGF signaling pathways in endochondral and intramembranous bone development and human genetic disease. Genes Dev. 16, 1446-1465.

Pritzker K.P., Gay S., Jimenez S.A., Ostergaard K., Pelletier J.P., Revell P.A., Salter D. and van den Berg W.B. (2006). Osteoarthritis cartilage histopathology: grading and staging. Osteoarthritis Cartilage 14, 13-29.

Schmitz N., Laverty S., Kraus V.B. and Aigner T. (2010). Basic methods in histopathology of joint tissues. Osteoarthritis Cartilage 18 (Suppl 3), S113-116.

Sharma A.R., Jagga S., Lee S.S. and Nam J.S. (2013). Interplay between cartilage and subchondral bone contributing to pathogenesis of osteoarthritis. Int. J. Mol. Sci. 14, 19805-19830.

Sophia Fox A.., Bdi A. and Rodeo S.A. (2009). The basic science of articulsr cartilage: Structure, composition and function. Sports Health 1, 461-568.

Zhang L., Hu J. and Athanasiou K.A. (2009). The role of tissue engineering in articular cartilage repair and regeneration. Crit. Rev. Biomed. Eng. 37, 1-57.

Accepted September 20, 2018